

Article

Synergistic Treatment of *Candida albicans* Infected Mice by AgNPs Synthesis *Penicillium chrysogenum*

Noor Naeem Jasim, Rasha M. A. Al-humairi, Teeba Hashim Mohammad*, and Ruwaida A. Hussein
Department of Biology, College of Science (for Women), University of Baghdad, Baghdad, Iraq.

*Correspondence: teebabiology@gmail.com

Available from: <http://dx.doi.org/10.21931/RB/CSS/2023.08.01.67>

Abstract: *Penicillium chrysogenum* has been used for the production of metal nanoparticles. It was experimentally shown that silver nitrate ions are reduced to silver nanoparticles in biomass, and silver nanoparticles are synthesized from 1 mM silver nitrate. The external morphology of ground AgNPs was established by SEM analysis and UV-visible spectrophotometry, and the size of AgNO₃ particles was observed to be 23 nm, with particles being spherical by AFM. *In vitro* investigations, the antifungal susceptibility of *Candida al* was calculated, and the results showed that the inhibitory effect of AgNPs synthesized with *P. chrysogenum* is increased with increasing the concentration of nanoparticles, and the effective fungicidal concentration (EC₅₀) was 1 ppm, and the minimum fungicidal concentration (MFC) was 100 ppm. Furthermore, the pathogenicity of *C. albicans* on kidneys in mice during infections was tested and thus indicated that the kidneys' ability was significantly enhanced when animals were treated with the combination of AgNPs and *P. chrysogenum*. This study's data from examination provide valuable preliminary statistics for using biosynthesized silver nanoparticles to manage various microorganisms.

Keywords: *Candida albicans*, AgNPs Synthesis, *Penicillium chrysogenum*

Introduction

Due to global public health, the widespread prevalence of conventional antifungal drugs is a significant threat^{1,2}. With the use of broad-spectrum conventional antibiotics and the increase in the infection rate in people with weakened immunity, they exacerbated their infection. They attenuated the possibility of a cure, especially with resistant fungi, which calls for improving treatments^{3,4}. Despite the improvement in antifungal drugs, the diseases caused by this type of yeast still cause intense symptoms and many deaths⁵. *C. albicans* is the most virulent and widespread species, accounting for approximately 50% of candidiasis, due to its ability to form biofilms and change their shape into multiple forms to adapt to the surrounding conditions^{6,7}. Therefore, it became necessary to search and find new treatments and innovations that are newer and more effective that work to defeat the diseases caused by these types of yeasts⁸.

In recent years, metallic nanoparticles have gained significant interest, especially with the development of the "green synthesis" method, which facilitates the synthesis process and the possibility of successful application to living organisms⁹. Nanoparticles have unique physiochemical properties that allow them to be used for various applications, including biological detection, drug delivery and anti-microbial drug¹⁰. Silver nanoparticles (AgNPs), which are known to be anti-

toxins, are the most prominent characteristics of these particles¹¹. AgNPs were first recognized when bacteria such as *E. coli* and *E. faecalis*¹² detected their anti-microbial effect. In recent years, AgNPs showed an antifungal activity when they combined with a microorganism¹³. When synthesized with fungal, silver nanoparticles increase the susceptibility to *C. albicans* compared to AgNPs alone¹⁴. Researchers were willing to discover new disinfection methods to act efficiently against pathogens. It has been previously recognized that metal nanoparticles, especially silver nanoparticles, display an inhibitory effect and anti-microbial activity at low units against a broad spectrum of fungi¹⁵. As a result of their efficiency on resistant strains of fungi, AgNPs are presented as the most potent conventional antifungal agents, among others. They are used in (bandages, wound healing ointments or creams, biomedical and surgical devices as disinfectants, textile coatings, and food packaging and storage)^{16,17}. These nanoparticles' small size and surface area allow them to have close contact with fungal membranes and display their fungicidal properties¹⁸. In animal models, several studies reported the incidence of *C. albicans* in cells and mice organs¹⁹. The data showed many studies conducted on the spots of ovarian infection within the organs of the mice body that stimulate the production of immune host cells in the living organism²⁰.

In this study, we used an experimental section of the kidney to demonstrate the efficacy of nanoparticles synthesized with fungi in treating systematic candidiasis infection in a mice model²¹.

Materials and Methods

Candida albicans isolation and manipulation

C. albicans, after isolation from patients, was incubated at a suspension density of 6×10^5 cells/mL for 3 h at 37°C in a tube containing 10% Bovine serum albumin. The portion of germ tube form (GTF) was assessed by light microscopy 400× magnification²².

Biomass production

For the production of *Penicillium chrysogenum* biomass, the culture was performed in a liquid broth consisting of (KH₂PO₄ 7.0g/L, K₂HPO₄ 2.0g/L, MgSO₄·7H₂O 0.1g/L, (NH₄)₂SO₄ 1.0g/L, yeast extract 0.6g/L and glucose 10g/L). The 500 ml flask was incubated for about 5 days at 25° C. Later incubation; the biomass was formed and harvested²³.

Synthesized of silver nanoparticles

We weighed 10 g of the produced biomass, and after washing to remove the rest of the media, it was inoculated into 200 mL of distilled water. The solution was incubated for about 3 days at room temperature. The produced biomass, after incubation, was again filtered by Whatmann No. 1 (filter paper), and silver nitrate particles were added at a concentration of 1 mM and incubated in the dark. A control positive contained only the fungal cell filtrate without AgNO₃²⁴.

Description of silver nanoparticles

The biosynthesis of silver nanoparticles was definite by measuring the absorption of the suspension using a (UV-Vis spectrophotometer). The production of silver nanoparticles was observed by a UV-visible Spectrophotometer, where a scan was done from 200-600 nm wavelengths²⁵.

After synthesis with the silver nanoparticles, the fungal cell filtrate was described using atomic force microscopy (AFM) to regulate the shape and size of AgNP synthesis. The characteristic of the AgNPs was studied using AFM and accomplished to determine the particle's height and mass by making a smear with the pellet. The external morphology of ground AgNPs was established by SEM analysis (ZEISS FE-SEM) ²⁶.

In Vitro Evaluation of Antifungal Activity

In Vitro, the antifungal activity of AgNPs was evaluated by dilution broth method. The suspension was diluted with sterile distilled water to get the final concentration of *C. albicans* after isolation from patients was used for this purpose. 200 ml of Sabouraud dextrose broth (SDB) liquid medium was prepared for yeast growth, and *C. albicans* were cultured for 72 h in the (SDB) medium before being used for examinations. Then, 10 μ L of this solution and AgNPs, prepared earlier, were added to test tubes containing 2 mL of (SDB) medium and incubated for 48 h at room temperature. Yeast medium with no AgNPs was measured as the negative control. The 10 μ L from the test tube was put in mueller-hinton agar Petri dishes, spread out by an L-shape rod and incubated for 48 h. Following that, suspension was placed on mueller-hinton agar containing different concentrations of the AgNPs, including sterile distilled water (as control) 1, 10, and 100 ppm. The plates were incubated in sterilized conditions, and the growth was observed ²⁷. To achieve reliable results, the experiment was done in triplicate. The antifungal activity for AgNPs was analyzed after images of plates were taken. In this study, MFC was investigated by sub-culturing broth microdilution of *C. albicans* from tubes yielding a negative yeast growth after incubation to define the number of colony-forming units (CFU) after 48 h of incubation ^{28,29}.

Data Analysis

The investigational data were statistically examined using ANOVA and one-tailed unpaired t-test for meaning testing, where $p < 0.05$ was measured as significant. Values are presented as the mean \pm SD of the three replications in each experiment ³⁰.

Animal model

Male mice aged 6 weeks weighing about 20 g were used in this study and had never been employed for any experimental techniques. 32 mice were vocally getting (100 mg/kg weight/d) for 30 days continuously divided into 4 groups:

- The control mice received normal saline.
- The control-positive mice were receiving AgNPs with *P. chrysogenum* only.
- The infected mice groups were receiving *C. albicans* only.
- The treatment mice groups were receiving *C. albicans* for 10 days and treatment by AgNPs with *P. chrysogenum* ³¹.

Kidney Tissues sections Preparation

Histological sections of kidney samples were prepared and fixed with formalin solution 10% for 24 h and then washed with running water and put in serial concentrations of the absolute alcohol ranging from 70% to 100% for 45 min. Each was cleared with (Xylene) for 45 min. And then placed in a mixture of xylene and paraffin wax at 58° C for infiltration for 15 min. The samples were

embedded in waxy molds for blocking and cutting by rotary microtome and using routine hematoxylin and eosin stains ³².

Photography: The slides were photographed with a Meije compound microscope with a camera.

Results

Candida albicans was isolated from the patients and designated for the biosynthesis of AgNPs. The harvested *P. chrysogenum* cells were incubated with AgNO₃ solution at a concentration of 1 mM and incubated in the dark at room temperature to the synthesis Gaps. Alteration in the reaction combination's color during incubation indicated the formation of AgNPs with *P. chrysogenum*. The reaction mixture color transformed to light brown after 3 days of incubation. In contrast, no change in color was detected in the control flasks (culture supernatant and 1 mM AgNO₃ solution only) in the similar experimental condition, showing no development The UV-Vis spectral examination of AgNPs suspension (AgNPs with *P. chrysogenum*) showed broadening spectrum with weak band at 445.5 and 466 nm, indicating absorption of the suspension synthesis of AgNPs using a (UV-Vis spectrophotometer, Figure 1.). By AFM analysis, SEM results showed spherical nanoparticles with an average size of 23 nm.

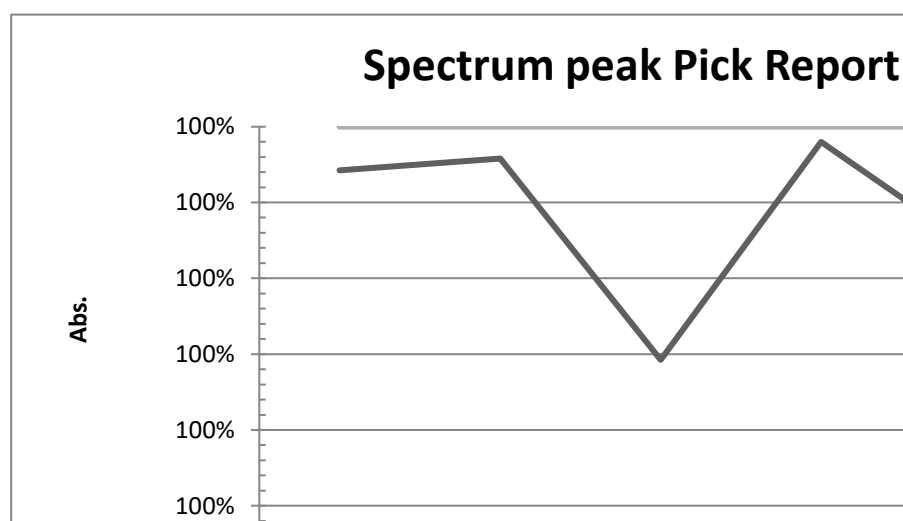


Figure 1. The UV-Vis spectrum of AgNPs suspension (AgNPs with *P. chrysogenum*)

In vitro calculation of antifungal activity

In vitro investigations were achieved to calculate the antifungal susceptibility of *C. albicans*. According to the results, the inhibitory effect of AgNPs synthesized with *P. chrysogenum* increased with increasing concentration of nanoparticles. The results showed that the effective fungicidal concentration (EC₅₀) was 1 ppm, and the minimum fungicidal concentration (MFC) was 100 ppm. In Figure 1, a comparison between the control sample and treatment sample at 1 ppm, 10 ppm and 100 ppm concentrations of AgNPs synthesized with *P. chrysogenum* suspensions, and the growth of *C. albicans* after 3 days on mueller-hinton culture medium Figure 2,3. The figures characterize the rate of AgNP synthesis on yeast growth inhibition in Table 1.

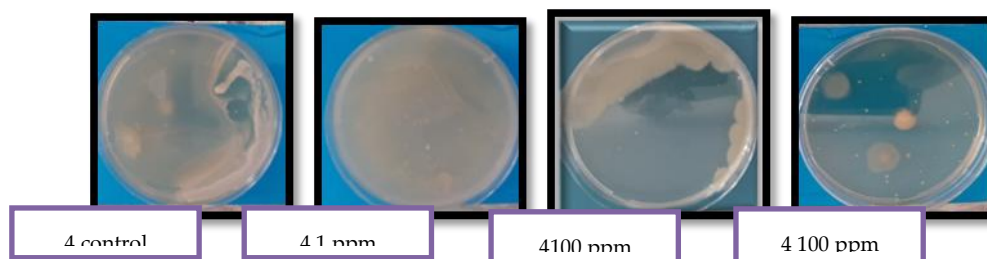


Figure 2. Effect of different concentrations of AgNPs Synthesized with *P. chrysogenum* on the growth of *C. albicans* after 3 days: control and treatments with AgNPs of 0 (as control) 1, 10, and 100 ppm concentrations, agar dilution method.

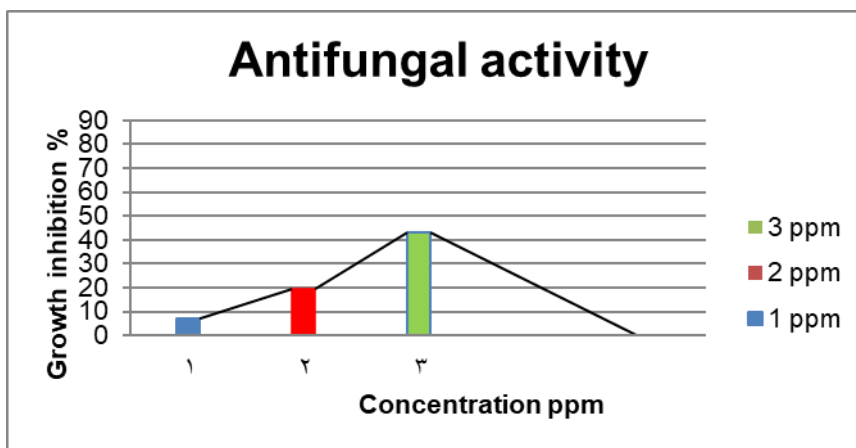


Figure 3. Growth inhibition percentage of *C. albicans* treated with different concentrations of the AgNPs Synthesized with *P. chrysogenum* for three days. Data are presented as a mean \pm SD of three replicates.

ppm (Concentration)	Diameter (mm)	Growth Inhibition %
Control	26.3 \pm 0.5	-
1	25.7 \pm 0.5	7.1
10	10.2 \pm 0.5	19.6
100	4.1 \pm 0.5	43.3

Table 1. Growth of *C. albicans* (growth diameter in mm) treated with several concentrations of AgNPs Synthesized with *P. chrysogenum* for 3 days. Data are referred to as a mean \pm SD of three replicates.

Histological dissecting of kidney

The results of these studies show that the infection was improved by treatment using AgNPs with *P. chrysogenum*. (Figure 4., A, B, C and D), a kidney from normal mice receiving normal saline (A), and the positive control mice were receiving AgNPs with *P. chrysogenum* only (B) after infection for 30 days with *Candida albicans* only (C). Treatment mice received *C. albicans* for 10 days and were treated with AgNPs with *P. chrysogenum* (D). The change occurred in the control kidney section. Figure 4. A showing normal renal cortex and Bowman's capsule with peripheral squamous epithelium (sq), glomerulus (GL), urinary space (US) and normal convoluted tubules (c). In Figure 4., B shows less necrosis and inflammatory cellular infiltration. (Fig. 4., C) showing diminished and

distorted glomeruli, leukocyte infiltration, edema exudate, necrotic foci, dilated tubules, abundant capsular space, infiltration of inflammatory cells surrounding the distorted glomeruli and tubules and interstitial edema. Vacuolated tubules and dark stained nuclei of the mesangial cells and vacuolations of the kidney tubules. The capillaries of most glomeruli appeared more congested, and slight edema of the tubular cells appeared in this group Figure 4., D.

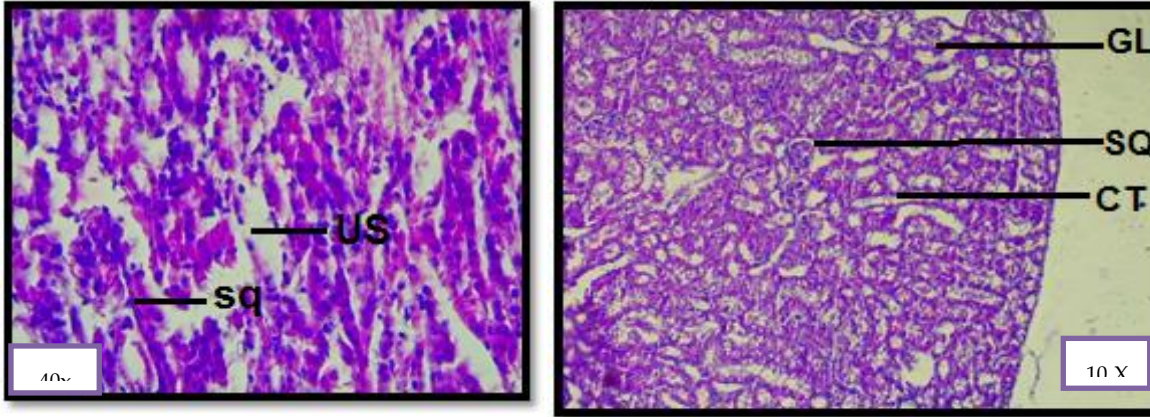


Figure 4 A. Histological section of normal kidney showing normal renal cortex and Bowman's capsule with peripheral squamous epithelium (SQ), glomerulus (GL), urinary space (US) and normal convoluted tubules (CT).

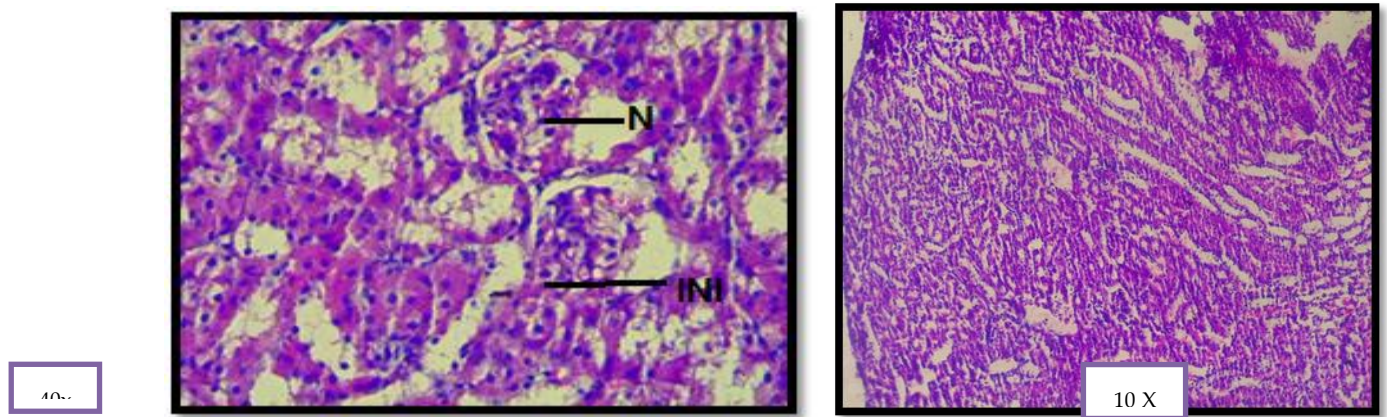


Figure 4 B shows less necrosis(N) and inflammatory cellular infiltration(INI).

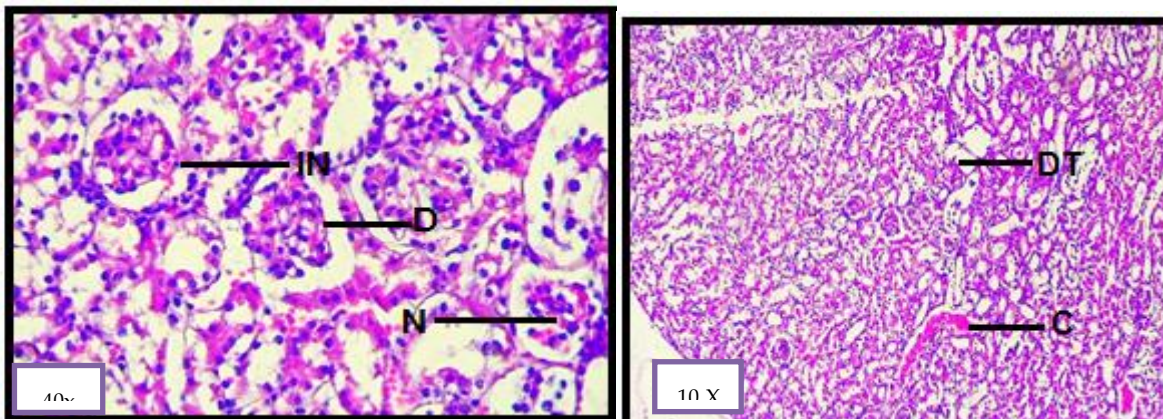


Figure 4 C shows diminished(D) and distorted glomeruli, leukocyte infiltration(IN), edema exudate (EE) and necrotic foci(NF), dilated tubules, abundant capsular space, infiltration of inflammatory cells surrounding the distorted glomeruli and tubules and interstitial edema. Vacuolated tubules and darkly stained nuclei of the mesangial cells and vacuolations of the kidney tubules. The capillaries of most glomeruli appeared more congested ©.

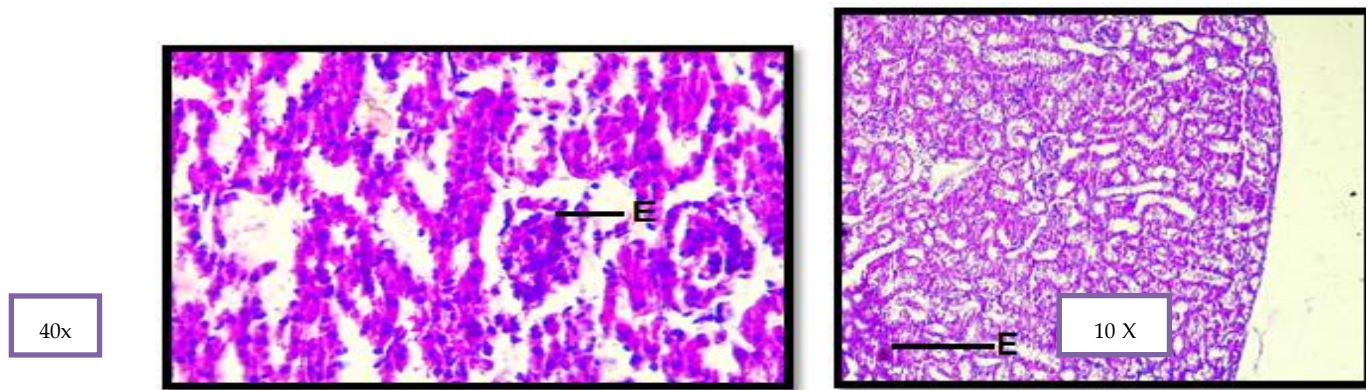


Figure 4 D. Slight edema(E) of the tubular cells appeared in this group.

Discussion

In vitro studies were done to determine the susceptibility of *C. albicans* and the antifungal activity of biosynthesized AgNPs with *P. chrysogenum* on *C. albicans*. Agar dilution methods studied the effect of different concentrations of AgNPs Synthesized with *P. chrysogenum* on the growth of *C. albicans*²³. The inhibitory effect of AgNPs increased with increasing the concentration of silver nanoparticles. The effective fungicidal concentration (EC50) was 1 ppm, and the minimum fungicidal concentration (MFC) was 100 ppm. The use of AgNPs as antifungal agents have been testified before. As in the case of,²⁴ informed that biosynthesized with a size of 23 nm were established to show antifungal activity against experimental yeast samples in the 1 to 100 ppm range during agar dilution method²⁴.

Nevertheless, there is no significant difference between the value size of the AgNPs informed by²⁴. According to the results, the mechanism of the therapeutic effect of silver nanoparticles could be shown as the interaction of (Ag^+ ions released from AgNPs) with the cell membrane of yeast leads to significant damage through the accumulation of ions in the interstitial places^{8,24,27}. In Figure 2, a dose-dependent method increased the growth inhibition percentage of *C. albicans* by AgNPs of 0,1, 10, and 100. This might be because of the high mass of silver nanoparticles at which the fungal medium can saturate and adhere to yeast to switch off pathogenic *Candida*³⁰. The lowest percentage was 100 ppm concentration, compared with 1 ppm as the effective concentration. Regardless of the values of inhibition percentage described in Table 1, it can be noticed that the AgNPs in the media affected the growth of *C. albicans* with a higher inhibition effect at 100 ppm concentration as the ratio reached 43.3 compared to 1 ppm concentration, which achieved 7.1, even though the mode action of the fungicidal effect of synthesized silver nanoparticles is quiet not understood. It has been suggested that the inhibition efficacy of AgNPs is due to the formation of pores on the yeast cell membrane, which ultimately leads to cell wall damage and cell death³¹.

Conclusions

C. albicans has been reserved as the main species related to human *Candida* infections; the standard investigational animal models for *Candida* species have also been fixed on *C. albicans*. However, many types of animals have been used to study yeast infections; the mice infection models employed the common for commercial reasons, easy treatment, and availability¹⁰. The use of biosynthesized AgNPs with *P. chrysogenum* as antifungal agents has been

described previously²⁵, illustrating that AgNPs with the size of 23 nm were established to show antifungal activity against tried yeast. The effective fungicidal concentration (EC50) was 1 ppm, and the minimum fungicidal concentration (MFC) was 100 ppm. Interestingly, our findings are consistent with the findings of Fátima et al.. However, our biosynthesized AgNPs with fungus are more effective antifungal agents against *Candida* infections, and our AgNPs with fungal significant alteration in antifungal activity may get up from the polydispersity and non-spherical shape of their AgNPs.³³ The study examinations are multifaceted and contain complex methods to measure the antifungal activity of AgNPs derived from "green" synthesis. These biogenic spherical and small AgNPs are persistent and established in vitro for an extended period and did not have a cytotoxic effect at concentrations that had an effective inhibitory result on (*C. albicans* growth, germ tube formation, hyphal growth and biofilm formation)³⁴. This may suggest that the combination of AgNPs and fungus could be an excellent therapeutic agent in the development of yeast infections³⁵.

Acknowledgements

The author thanks the Ministry of Science and Technology Research and the University of Baghdad for technical support.

References

1. Lima, S.L., Colombo, A.L., de Almeida, J.N. Fungal Cell Wall: Emerging Antifungals and Drug Resistance. *Front Microbiol.* 10:9. DOI:10.3389/fmicb.2019.02573.
2. Duval C et al., The adaptive response to iron involves changes in energetic strategies in the pathogen *Candida albicans*. *Microbiologyopen*, DOI: 10.1002/mbo3.970.
3. Goffeau A. Drug resistance - The fight against fungi. *Nature.* 2008;452(7187):541–2. DOI:10.1038/452541a.
4. Hendrickson JA, et al. Antifungal Resistance: a Concerning Trend for the Present and Future. *Current Infectious Disease Reports.* 2019;21(12):8. DOI:10.1007/s11908-019-0702-9.
5. Xiao ZL, et al. Epidemiology, species distribution, antifungal susceptibility and mortality risk factors of candidemia among critically ill patients: a retrospective study from 2011 to 2017 in a teaching hospital in China. *Anti-microbial Resistance Infection Control.* 2019;8:7. DOI:10.1186/s13756-019-0534-2.
6. Kadosh D. Regulatory mechanisms controlling morphology and pathogenesis in *Candida albicans*. *Current Opinion In Microbiology.* 2019. 52: p. 27–34 DOI: 10.1016/j.mib.2019.04.005.
7. Naglik JR, Gaffen SL, Hube B. Candidalysin: discovery and function in *Candida albicans* infections. *Current Opinion In Microbiology.* 2019;52:100–9. DOI:10.1016/j.mib.2019.06.002.
8. Feng WL, et al. Regulatory Role of ERG3 and Efg1 in Azoles-Resistant Strains of *Candida albicans* Isolated from Patients Diagnosed with Vulvovaginal Candidiasis. *Indian Journal Of Microbiology.* 2019;59(4):514–24. DOI:10.1007/s12088-019-00833-x.
9. Nisar P, et al. Anti-microbial activities of biologically synthesized metal nanoparticles: an insight into the mechanism of action. *Journal Of Biological Inorganic Chemistry.* 2019;24(7):929–41. DOI:10.1007/s00775-019-01717-7.
10. Hirpara DG, Gajera HP. Green synthesis and antifungal mechanism of silver nanoparticles derived from chitin- induced exometabolites of *Trichoderma interfusant*. *Applied Organometallic Chemistry*: p. 15 DOI: 10.1002/aoc.5407.
11. Lakhani P, et al. Optimization, stabilization, and characterization of amphotericin B-loaded nanostructured lipid carriers for ocular drug delivery—*International Journal Of Pharmaceutics.* 2019;572:14. DOI:10.1016/j.ijpharm.2019.118771.

12. Sardella D, Gatt R, Valdramidis VP. Metal nanoparticles for controlling fungal proliferation: quantitative analysis and applications. *Current Opinion In Food Science*. **2019**;30:49–59. DOI:10.1016/j.cofs.2018.12.001.
13. Rai M, Yadav A, Gade A. Silver nanoparticles as a new generation of anti-microbials. *Biotechnol Adv*. 2009;27(1):76–83. DOI:10.1016/j.biotechadv.2008.09.002.
14. Rai MK, et al. Silver nanoparticles: the powerful nano weapon against multidrug-resistant bacteria. *Journal Of Applied Microbiology*. **2012**;112(5):841–52. DOI:10.1111/j.1365-2672.2012.05253.x.
15. Ebrahiminezhad A, et al. Green synthesis and characterization of nanoparticles using *Alcea rosea* flower extract as a new generation of anti-microbials. *Chemical Industry Chemical Engineering Quarterly*. **2017**;23(1):31–7. DOI:10.2298/ciceq150824002e.
16. Zheng KY, et al. Anti-microbial silver nanomaterials. *Coord Chem Rev*. 2018;357:1–17. DOI:10.1016/j.ccr.2017.11.019. Page 15/20.
17. Prasad K, et al. Synergic bactericidal effects of reduced graphene oxide and silver nanoparticles against Gram-positive and Gram-negative bacteria. *Sci Rep*. **2017**;7:11. DOI:10.1038/s41598-017-01669-5.
18. Wypij M, et al. Silver nanoparticles from *Pilimelia columellifera* subsp *pallida* SL19 strain demonstrated antifungal activity against fungi causing superficial mycoses. *Journal Of Basic Microbiology*. **2017**;57(9):793–800. DOI:10.1002/jobm.201700121.
19. Balashanmugam P, et al. Phytogenic synthesis of silver nanoparticles, optimization and evaluation of in vitro antifungal activity against human and plant pathogens. *Microbiol Res*. **2016**;192:52–64. DOI:10.1016/j.micres.2016.06.004.
20. Hussain MA, et al. Combination Therapy of Clinically Approved Antifungal Drugs Is Enhanced by Conjugation with Silver Nanoparticles. *Int Microbiol*. **2019**;22(2):239–46. DOI:10.1007/s10123-018-00043-3.
21. 21. Chaves G. M., de Q Cavalcanti M. A., Carneiro-Leao A. M. A., and Lopes S. L., Model of experimental infection in healthy and immunosuppressed Swiss albino mice (*Mus musculus*) using *Candida albicans* strains with different patterns of enzymatic activity. *Brazilian Journal of Microbiology*. **2004**;35(4): 324–329.
22. 22. Abass N, Shanan Z, Mohammed T, Abbas L. Fabricated of Cu Doped ZnO Nanoparticles for Solar Cell Application. *Baghdad Science Journal*, **2018**;15:2. <http://dx.doi.org/10.21123/bsj.2022.19.1.0217>.
23. 23. El-Moslamy S. H., Elkady M. F., Rezk A. H., and Abdel-Fattah Y. R. Applying Taguchi design and large-scale strategy for mycosynthesis of nanosilver from endophytic *Trichoderma* 24. *harzianum* SYA.F4 and its application against phytopathogens. *Sci. Rep*. **2017**; 7:45297.
24. 25. Fátima, F., Verma, S. R., Pathak, N., and Bajpai, P. Extracellular biosynthesis of silver nanoparticles and their microbicidal activity. *J. Glob. Antimicrob. Resist*. **2016**; 7, 88–92.
25. 26. Hamed, S., Ghaseminezhad, M., Shokrollahzadeh, S., and Shojaosadati, S. A. Controlled biosynthesis of silver nanoparticles using nitrate reductase enzyme induction of filamentous fungus and their antibacterial evaluation. *Artif. Cells Nanomed. Biotechnol*. **2017**; 45, 1588–1596.
26. 27. Velusamy, P., Kumar, G. V., Jeyanthi, V., Das, J., and Pachaiappan, R. Bio-inspired green nanoparticles: synthesis, mechanism, and antibacterial application. *Toxicol. Res*. **2016**; 32, 95–102.
27. 28. Schaller M, Borelli C, Korting HC and Hube B: Hydrolytic enzymes as virulence factors of *Candida albicans*. *Mycoses* 48: 365-377, **2005**.
28. 29. Kumamoto CA and Vences MD: Contributions of hyphae and hypha-co-regulated genes to *Candida albicans* virulence. *Cell Microbiol* 7: 1546-1554, **2005**.
29. Chairman W, Burrows T, Cooper S, Crookes Jackson, P Kowalczyk, G Lewis, Lipworth S, Lohmann DH, Sanderson Watts, Whitehead S. In vivo test methods to identify the acute toxicity estimate (ate) alternative test method to the LD50 test. Produced by a working party of the Environment, *Health and Safety Committee (EHSC) of the Royal Society of Chemistry*, **2013**; (4): 1-5.
30. 30. Romani, L., A. Menacacci, E. Cenci, R. Spaccapelo, P. Mosci, P. Puccetti, and F. Bistoni. CD41 subset expression in murine candidiasis. *J. Immunol*. **1993**; 150:925.
31. 31. Cui JH, et al. Synergistic combinations of antifungals and anti-virulence agents to fight against *Candida albicans*. *Virulence*. **2015**;6(4):362–71. DOI:10.1080/21505594.2015.1039885.
32. 32. Shareef AA, Hassan ZA, Kadhim MA and Al Mussawi AA. Antibacterial Activity of Silver Nanoparticles Synthesized by Aqueous Extract of *Carthamus Oxycantha* M.Bieb. Against Antibiotics Resistant

- Bacteria. *Baghdad Science Journal*. **2022**; 19(3): 460-468. <http://dx.doi.org/10.21123/bsj.2022.19.3.0460>.
33. 33. Sardella D, Gatt R, Valdramidis VP. Metal nanoparticles for controlling fungal proliferation: quantitative analysis and applications 2019. *Current Opinion In Food Science*. 30:49–59. DOI:10.1016/j.cofs.2018.12.001.
34. 34. Radhakrishnan VS, et al. Silver nanoparticles induced alterations in multiple cellular targets, critical for drug susceptibilities and pathogenicity in fungal pathogens (*Candida albicans*). *Int J Nanomed*. **2018**;13:2647–63. DOI:10.2147/ijn.s150648.
35. 35. Neto JBD, et al. Action mechanism of naphthofuranquinones against fluconazole-resistant *Candida tropicalis* strains evidenced by proteomic analysis: The role of increased endogenous ROS. *Microb Pathog*. **2018**;117:32–42. DOI:10.1016/j.micpath.2017.12.016.

Received: May 15, 2023/ Accepted: June 10, 2023 / Published: June 15, 2023

Citation: Jasim , N.N.; Al-humairi,R.M.A.; Mohammad ,T.H.; Hussein ,R.A. Synergistic Treatment of *Candida albicans* Infected Mice by AgNPs Synthesis *Penicillium chrysogenum*. *Revis Bionatura* 2023;8 (1) 67. <http://dx.doi.org/10.21931/RB/CSS/2023.08.01.67>